Brazilian Journal of Medical and Biological Research (1997) 30: 1135-1144
ISSN 0100-879X

Myocyte necrosis is the basis for fibrosis in renovascular hypertensive rats

M.P. Okoshi[1], L.S. Matsubara[1], M. Franco[2], A.C. Cicogna[1] and B.B. Matsubara[1]

[1]Departamento de Clínica Médica and [2]Departamento de Patologia, Faculdade de Medicina de Botucatu, Universidade Estadual Paulista, Botucatu, SP, Brasil

Abstract

The pathogenesis of fibrosis and the functional features of pressure overload myocardial hypertrophy are still controversial. The objectives of the present study were to evaluate the function and morphology of the hypertrophied myocardium in renovascular hypertensive (RHT) rats. Male Wistar rats were sacrificed at week 4 (RHT4) and 8 (RHT8) after unilateral renal ischemia (Goldblatt II hypertension model). Normotensive rats were used as controls. Myocardial function was analyzed in isolated papillary muscle preparations, morphological features were defined by light microscopy, and myocardial hydroxyproline concentration (HOP) was determined by spectrophotometry. Renal artery clipping resulted in elevated systolic arterial pressure (RHT4: 178 ± 19 mmHg and RHT8: 194 ± 24 mmHg, $P<0.05$ *vs* control: 123 ± 7 mmHg). Myocardial hypertrophy was observed in both renovascular hypertensive groups. The myocardial HOP concentration was increased in the RHT8 group (control: 2.93 ± 0.38 µg/mg; RHT4: 3.02 ± 0.40 µg/mg; RHT8: 3.44 ± 0.45 µg/mg of dry tissue, $P<0.05$ *vs* control and RHT4 groups). The morphological study demonstrated myocyte necrosis, vascular damage and cellular inflammatory response throughout the experimental period. The increased cellularity was more intense in the adventitia of the arterioles. As a consequence of myocyte necrosis, there was an early, local, conjunctive stroma collapse with disarray and thickening of the argyrophilic interstitial fibers, followed by scarring. The functional data showed an increased passive myocardial stiffness in the RHT4 group. We conclude that renovascular hypertension induces myocyte and arteriole necrosis. Reparative fibrosis occurred as a consequence of the inflammatory response to necrosis. The mechanical behavior of the isolated papillary muscle was normal, except for an early increased myocardial passive stiffness.

Correspondence
M.P. Okoshi
Departamento de Clínica Médica
Faculdade de Medicina de Botucatu
UNESP
18618-000 Botucatu, SP
Brasil
Fax: 55 (014) 822-2238

Publication supported by FAPESP.

Received November 27, 1996
Accepted July 8, 1997

Key words
- Coronary vascular remodeling
- Myocardial function
- Pressure overload hypertrophy
- Papillary muscle
- Reparative fibrosis

Introduction

Myocardial hypertrophy is an adaptive response to ventricular overload. Although there has been considerable investigation on myocardial function with pressure overload hypertrophy, the functional features of the myocardium remain controversial; mechanical activity has been reported to be increased (1,2), unchanged (3-5), or depressed (6,7). Changes in myocyte and/or interstitial components of the myocardium have been pointed out as the causes of cardiac dysfunction (8-10). Interstitial collagen accumulation occurs in various experimental models of pressure overload myocardial hypertrophy (10-14) and has been associated with myocardial dysfunction by many authors (8,10-13). However, others have failed to demonstrate an association between fibrosis and cardiac muscle dysfunction (15).

Another matter of disagreement among the studies is about the pathogenetic origin of myocardial fibrosis. Weber et al. (8,16) have hypothesized that the fibrosis occurring in pressure overload hypertrophy might be both reparative and reactive. In the former case, myocyte necrosis may initiate collagen deposition and lead to replacement scarring. Studies (17-19) have demonstrated that either renovascular or angiotensin II (AII)-induced hypertension causes cardiomyocyte necrosis followed by fibrosis. In addition, vascular injury is the basis of patchy multifocal myocardial necrosis and scarring in hypertensive rats with aortic banding (20). On the other hand, reactive fibrosis is defined as the result of an increased collagen synthesis by the AII-stimulated interstitial fibroblasts, with no cell loss (8). Accordingly, an excessive accumulation of collagen in the hypertrophied myocardium of rats with renovascular hypertension or aortic constriction has been described with no evidence of myocyte necrosis (12,21). Under some experimental conditions, both types of fibrosis might occur sequentially as reported for unilateral renal ischemia (22).

To further address this issue, we analyzed the pathogenesis of myocardial fibrosis in renovascular hypertensive rats and evaluated the influence of fibrosis on mechanical performance of papillary muscles. We demonstrated that the myocardial fibrosis was always related to myocyte necrosis, suggesting rather a reparative than a reactive fibrosis. There were an early collapse and disarray of the reticular stroma in the areas of myocyte loss and a later replacement by fibrosis. Regardless of the remarkable morphological changes, the functional behavior of the papillary muscles was close to normal, except for an early transitory increase in myocardial stiffness.

Material and Methods

Animal and groups

Eight-week old male Wistar rats weighing 130 to 170 g were anesthetized *ip* with thiopental sodium (50 mg/kg). Renovascular hypertension (RHT) was induced by constricting the left renal artery to an outer diameter of 0.25 mm with the aid of a silver clip. The contralateral kidney was untouched (Goldblatt II hypertension model). All animals were housed in a temperature-controlled room (24°C) on a 12-h light/dark cycle, and food and water were supplied *ad libitum*.

The rats were sacrificed 4 weeks (RHT4 group, N = 15) or 8 weeks (RHT8 group, N = 15) after surgery. Results were compared to sex-matched 14-week old rats (control group, N = 15). Before sacrifice, systolic arterial pressure (SAP) was measured in all animals using a tail cuff.

Functional study

Ten animals from each group were sacrificed by decapitation for functional study. The hearts were quickly removed and placed in oxygenated Krebs-Henseleit solution at 28°C. Trabecular carneae or papillary muscles

were dissected from the left ventricle (LV), mounted between two spring clips, and placed vertically in a chamber containing Krebs-Henseleit solution at 28°C and gassed with 95% O_2 and 5% CO_2. The composition of the Krebs-Henseleit solution was as follows: 118.5 mM NaCl, 4.69 mM KCl, 2.52 mM $CaCl_2$, 1.16 mM $MgSO_4$, 1.18 mM KH_2PO_4, 5.50 mM glucose, and 25.88 mM $NaHCO_3$. The lower spring clip was attached to a Kyowa model 12OT-2OB force transducer by a thin steel wire (1/15,000 inch) which passed through a mercury seal at the bottom of the chamber. The upper spring clip was connected by a thin steel wire to a rigid lever arm above which a micrometer stop was mounted for the adjustment of muscle length. The lever arm was made of magnesium with a ball-bearing fulcrum and a lever arm ratio of 4:1. A displacement transducer (Hewlett-Packard, 7 DCDT-50) was mounted above the short end of the lever arm. Preparations were stimulated 12 times/min with 5-ms square wave pulses through parallel platinum electrodes, at voltages 10% greater than the minimum required to produce a maximal mechanical response.

The muscles were kept contracting isotonically with light loads for 60 min and then loaded to contract isometrically and stretched to the maximum of their length-tension curves.

After a 5-min period in afterloaded isotonic contractions, muscles were again placed under isometric conditions, and the peak of the length-tension curve (L_{max}) was carefully determined. A 15-min period of stable isometric contraction was imposed prior to the experimental period and one isometric contraction was then recorded. The isotonic contraction parameters were obtained using the lightest preload able to maintain L_{max}. The passive length-tension curves were derived from data obtained at lengths of 90%, 92%, 94%, 96%, 98% and 100% of L_{max}.

The following parameters were measured from isometric contractions: peak developed tension (DT; g/mm^2), resting tension (RT; g/mm^2), time to peak tension (TPT; ms), maximum rate of tension development (+dT/dt; g/mm^2/s), maximum rate of tension decline (-dTdt; g/mm^2/s) and time for tension to fall from peak to 50% of peak tension (RT_{50}; ms). For isotonic contractions, the following parameters were assessed: peak shortening (PS; mm), time to peak shortening (TPS; ms), maximum velocity of isotonic shortening (+dL/dt; muscle length/s), maximum velocity of isotonic relengthening (-dL/dt; muscle length/s) and relative variation of length [(L_{max} - PS)/L_{max}].

At the end of each experiment, the muscle length at L_{max} was measured and the muscle between the two clips was blotted dry and weighed. Cross-sectional areas were calculated from the muscle weight and length by assuming cylindrical uniformity and a specific gravity of 1.0. All force data were normalized for the muscle cross-sectional area and length data were normalized by the muscle length (L_{max}).

Biochemical study

Hydroxyproline (HOP) was measured in tissue obtained from the LV apex according to the method described by Switzer (23). Briefly, the tissue was dried for 4 h using an SC 100 SpeedVac Concentrator attached to a TR 100 refrigerated condensation trap and a VP 100 vacuum pump (Savant Instruments Inc., Farmingdale, NY). Tissue dry weight was determined and the samples were hydrolyzed overnight at 110°C with 6 N HCl (1 ml/10 mg dry tissue). An aliquot of 50 µl of the hydrolysate was transferred to an Eppendorf tube and dried in the SpeedVac Concentrator. One ml of deionized water was added and the sample was transferred to a tube with a teflon screw-on cap. One ml of potassium borate buffer, pH 8.7, was added to maintain a constant pH and the sample was oxidized with 0.3 ml of chloramine T solution at room temperature for exactly 20

min. The addition of 1 ml of 3.6 M sodium thiosulfate with thorough mixing for 10 s stopped the oxidation process. The solution was saturated with 1.5 g KCl and the tubes were capped and heated in boiling water for 20 min. After cooling to room temperature, the aqueous layer was extracted with 2.5 ml toluene. One ml of toluene extract was transferred to a 12 x 75-mm test tube and 0.4 ml of Ehrlich's reagent was added to allow the color to develop for 30 min. Absorbances were read at 565 nm against a reagent blank. Deionized water and 20 µg/ml HOP were used as blank and standard, respectively.

Morphological study

Five animals from each group were sacrificed for morphological study. Hearts were excised and the ventricles separated, weighed and fixed in 10% buffered formalin for 24 h. Formalin-fixed tissue was serially dehydrated and embedded in paraffin; serial 5-µm thick sections were stained with hematoxylin and eosin, Sirius Red F3BA or silver for reticular fibers. Histological indicators of myocardial necrosis were the presence of muscle cells with no nuclei or cross striation, alongside with local accumulation of inflammatory cells and confluence of fibrotic tissue.

Statistical analysis

All grouped data are reported as means ± SD and compared by one-way analysis of variance and the *post hoc* Tukey test. The normalized LV and right ventricular (RV) weights were analyzed by the nonparametric Kruskal-Wallis test.

Prior to comparing the diastolic length-tension relationship for the three groups, the resting tension at L_{90} was subtracted from all subsequent tension data in each experiment in order to have all length-tension curves intercepting the Y axis origin at L_{90}. The diastolic length (L)-tension (RT) curves for the 3 groups were fitted to mono-exponential relations of the form $RT = A[e^{B(L-L_0)} - 1]$, where A and B are fitting parameters, and L_0 is the muscle length corresponding to zero resting tension. These nonlinear relations were compared by constructing an F ratio from the residual sum of squares (24). This test determines whether separate fits to data from two groups are significantly better than the combined fit to all data from two groups. Accordingly, a significant F ratio indicates that the two sets of data being compared were significantly different from each other. For all comparisons, statistical significance was taken to be $P<0.05/k$, where k is the number of comparison.

Results

The mean values obtained for the morphometric parameters, SAP and myocardial HOP concentration for all groups are summarized in Table 1.

Renal artery clipping resulted in an increased SAP (RHT4: 178 ± 19 mmHg and RHT8: 194 ± 24 mmHg, $P<0.05$ *vs* control: 123 ± 7 mmHg). Analysis of the hypertrophy index, expressed by left or right ventricular/body weight ratio, showed a significant LV hypertrophy after 4 weeks of RHT, which remained unchanged after 8 weeks. There was no RV hypertrophy in the RHT groups. Myocardial HOP concentration was significantly increased only after 8 weeks of RHT (control: 2.93 ± 0.38 µg/mg; RHT4: 3.02 ± 0.40 µg/mg; RHT8: 3.44 ± 0.45 µg/mg dry tissue, $P<0.05$ *vs* control and RHT4).

Tables 2 and 3 respectively show the isometric and isotonic contraction data of the papillary muscles. There was no significant difference among groups. Figure 1 shows the mean curves for the passive length-tension relations for all groups. Statistical analysis demonstrated a significant shift to the left of the relations in the RHT4 group, indicating increased passive myocardial stiffness compared to controls.

In contrast to the almost normal func-

tional behavior, the histological study showed striking arterial and myocardial lesions in both ventricles in the RHT groups (Figures 2 and 3). Myocardial histology was normal in control animals. After 4 weeks of renal ischemia, there were scattered foci of myocyte necrosis of different sizes. The necrotic process comprised one single cell or groups of myocytes (Figure 2A). The cell necrosis induced a predominantly lymphomononuclear inflammatory response with few polymorphonuclear neutrophils. Collapse of the reticular framework occurred at the sites of myocyte loss as demonstrated by silver staining (Figure 2B), as well as accumulation of inflammatory cells. In addition, segmental medial hypertrophy, hyalinization and fibrinoid necrosis of the intramural coronary arteries were observed. Many arteries presented adventitial lymphomononuclear inflammatory exudate and edema (Figure 2C). In the RHT8 group, the areas of myocardial necrosis were more frequent and larger. Recent myocyte necrosis was found in combination with foci of reparative fibrosis and healing. After eight weeks of renal ischemia, the changes of the intramural coronary arteries were more striking. The adventitial inflammatory process involved the adjacent myocytes and was accompanied by increased perivascular and interstitial fibrosis and scarring (Figure 3A,B).

Discussion

This study demonstrated that rats with left ventricular hypertrophy due to renovascular hypertension presented marked morphological alterations, such as myocyte necrosis, vascular damage and interstitial fibrosis.

The presence of cardiomyocyte necrosis has been previously described in the present experimental model (19). In rats with RHT, the myocyte injury and necrosis have been attributed to the resulting abnormal increase of the renin-angiotensin system activity, sys-

Table 1 - Group comparisons of systolic arterial pressure (SAP), morphometric parameters and myocardial hydroxyproline concentration (HOP).

Data are reported as means ± SD for N = 15. BW, Body weight; LVW, left ventricle weight; RVW, right ventricle weight; L_{max}, muscle length at peak of developed tension; CSA, cross-sectional area; RHT4, renovascular hypertension for 4 weeks; RHT8, renovascular hypertension for 8 weeks. *P<0.05 *vs* control group; #P<0.05 *vs* RHT4 group (one-way analysis of variance and *post hoc* Tukey test).

	Control	RHT4	RHT8
SAP (mmHg)	123 ± 7	178 ± 19*	194 ± 24*
BW (g)	323 ± 20	274 ± 22*	356 ± 43#
LVW/BW (mg/g)	2.01 ± 0.13	2.69 ± 0.32*	2.73 ± 0.33*
RVW/BW (mg/g)	0.64 ± 0.08	0.71 ± 0.08	0.68 ± 0.10
L_{max} (mm)	6.30 ± 0.93	5.90 ± 0.66	6.53 ± 0.71
CSA (mm^2)	0.82 ± 0.20	0.82 ± 0.23	0.84 ± 0.19
HOP (µg/mg)	2.93 ± 0.38	3.02 ± 0.40	3.44 ± 0.45*#

Table 2 - Isometric contraction data.

Data are reported as means ± SD for N = 10. DT, Peak developed tension; RT, resting tension; TPT, time to peak tension; +dT/dt, maximum rate of tension development; -dT/dt, maximum rate of tension decline; RT_{50}, time for tension to fall from peak to 50% of peak tension; RHT4, renovascular hypertension for 4 weeks; RHT8, renovascular hypertension for 8 weeks (one-way analysis of variance and *post hoc* Tukey test).

	Control	RHT4	RHT8
DT (g/mm^2)	8.59 ± 2.12	8.95 ± 2.50	8.24 ± 1.92
RT (g/mm^2)	0.80 ± 0.24	0.87 ± 0.30	0.77 ± 0.33
TPT (ms)	201 ± 16	201 ± 10	205 ± 15
+dT/dt ($g/mm^2/s$)	76 ± 21	82 ± 29	74 ± 20
-dT/dt ($g/mm^2/s$)	19 ± 5.6	21 ± 5.2	20 ± 4.1
RT_{50} (ms)	310 ± 57	278 ± 39	276 ± 36

Table 3 - Isotonic contraction data.

Data are reported as means ± SD for N = 10. PS, Peak shortening; TPE, time to peak shortening; +dL/dt, maximum velocity of isotonic shortening; -dL/dt, maximum velocity of isotonic relengthening; ML, muscle length; $(L_{max} - PS)/L_{max}$, relative variation of length; L_{max}, muscle length at peak of developed tension; RHT4, renovascular hypertension for 4 weeks; RHT8, renovascular hypertension for 8 weeks (one-way analysis of variance and *post hoc* Tukey test).

	Control	RHT4	RHT8
PS (mm)	1.70 ± 0.46	1.53 ± 0.18	1.73 ± 0.41
TPE (ms)	215 ± 18	218 ± 14	223 ± 21
+dL/dt (ML/s)	2.45 ± 0.52	2.28 ± 0.41	2.46 ± 0.72
-dL/dt (ML/s)	4.36 ± 1.24	3.97 ± 1.08	3.92 ± 1.35
$(L_{max} - PS)/L_{max}$	0.73 ± 0.04	0.74 ± 0.03	0.73 ± 0.06

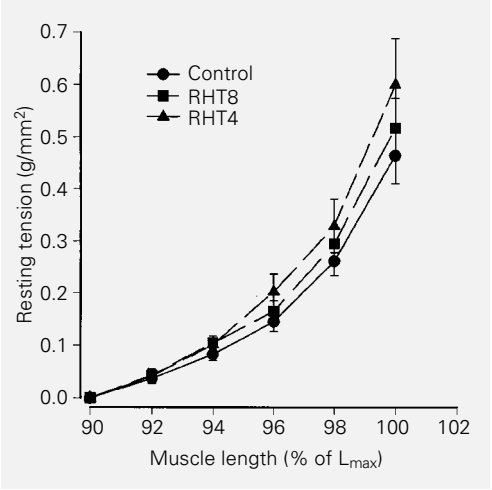

Figure 1 - Passive length-tension relations for renovascular hypertension at 4 (RHT4 group) and 8 weeks (RHT8 group) and for control rats (control group). Results are reported as means ± SD. The curve for the RHT4 group was significantly different from the curve for the control group ($P<0.05$) (nonlinear regression modeling comparing parameters estimated by the residual sum of squares, F ratio test). The shift to the left indicates increased myocardial passive stiffness. L_{max}: muscle length at peak of developed tension.

temic or local (19,25), and to the coronary vascular damage (20). The toxic effect of AII on the myocardium is thought to be due to its direct action or to the AII-stimulated catecholamine release (19,26).

Our findings of lymphomononuclear inflammatory accumulation around the foci of necrosis and around the arteries in both the RHT4 and RHT8 groups suggest a sustained injury to the myocardium throughout the follow-up period. This is not in accordance with other investigators (17,18), who showed that the necrotic damage after a chronic increase in plasma AII levels was limited to the first two days, despite a continued increase in plasma AII levels. Kabour et al. (18,19) showed that the AII-induced myocyte necrosis is mediated by the angiotensin type 1 receptor and speculated that a chronic increase in circulating AII may cause receptor downregulation protecting the myocardium against further AII-mediated necrosis (18). The different experimental approaches, RHT and AII infusion, may explain the discrepant results and further studies are needed for a better understanding of this point.

Another possible mechanism for multifocal myocyte necrosis is myocardial ischemia due to a coronary artery abnormality. In hypertensive rats with aortic banding, myocyte and arterial necrosis and scarring have been reported up to the sixth week of follow-up (20). There was a close association between arterial and myocardial lesions, suggesting that muscle necrosis and scars were due to ischemia. Our findings of arteriole damage, perivascular edema and cellular inflammatory response may support this hypothesis. The presence of inflammatory cells within the adventitia of intramyocardial coronary vessels has been reported by others (27). It was suggested that the production of mediators by those cells might contribute to the fibrous tissue response. Besides the vascular wall injury and the inflammatory response, other mechanisms might be involved in the perivascular edema and fibrosis. It has been reported that activation of the renin-angiotensin system is related to increased coronary vascular permeability (28-31). This vascular dysfunction may be the result of increased release of nitric oxide (30), bradykinin and prostaglandins (31). Our study indicates that, in addition to changes in arteriolar permeability, cell necrosis and the subsequent inflammatory response are associated with perivascular fibrosis.

In the present study, since myocyte necrosis was found to be so variable, restricted to one single cell or involving a large group of cells, the pattern of the subsequent fibrosis also presented variable characteristics. Collagen accumulation was observed in delicate septa between muscle cells or in large scars. In our interpretation, the late perivascular and interstitial myocardial fibrosis was reparative. The fibrosis replaced areas of myocyte loss or arterial smooth muscle cell damage. The stromal collapse reinforced this interpretation. This suggestion is in disagreement with the hypothesis of reactive fibrosis occurring in RHT (8,16), which was based on the absence of inflammatory cells near the sites of myocardial fibrosis (12,21). As observed in the present study, Hinglais et al. (14) found increased myocardial fibrosis in hypertensive rats closely related to the presence of lymphocytes and macrophages

around degenerative, myocytolytic muscle cells, indicating that the myocardial fibrosis was a reparative process. In contrast, Campbell et al. (22) described inflammatory cells in the cardiac tissue only during the few days following the induction of unilateral renal ischemia in rats. Nevertheless, they observed progressive fibrosis until the eighth week of RHT, which suggested that a mechanism other than cell necrosis was the agent of abnormal collagen accumulation.

These different results in morphological patterns might have been due to variations introduced in the classical Goldblatt model of RHT. In order to produce renal ischemia, the authors promoted aortic constriction including the right renal artery (21,22), or both renal arteries (20). These technical variations may induce different degrees of hormonal release and consequently different degrees of heart damage.

Our hypothesis for myocardial fibrosis is summarized in Figure 4. The activation of the renin-angiotensin system by unilateral renal ischemia causes arterial hypertension, myocardial hypertrophy, myocyte necrosis and a perivascular inflammatory response. Myocardial hypertrophy is further stimulated by pressure overload and increases myocardial oxygen consumption, with oxygen delivery possibly being impaired by the perivascular inflammatory process. All of these factors, taken together, result in myocardial hypoxemia and further cell necrosis. Myocyte necrosis initiates the healing process, which ends with fibrosis replacement.

The results about the mechanical function of isolated papillary muscles did not show a depressed systolic function in spite of the remarkable morphological changes. In fact, there was a disagreement between myocardial function and the intensity of morphological damage. Other authors have observed the same behavior. Conrad et al. (32) found significant functional changes in the papillary muscles of spontaneously hypertensive rats only when there was heart failure in rats.

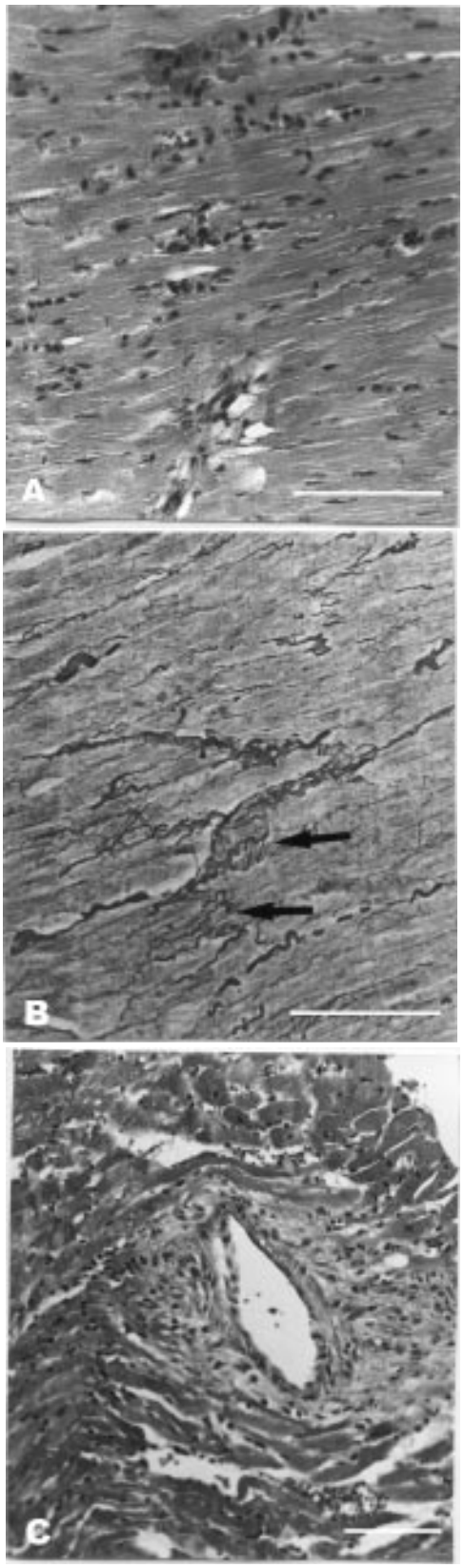

Figure 2 - Photomicrographs of myocardium from a renovascular hypertensive rat sacrificed after 4 weeks of left renal artery clipping. *Panel A*, Tissue stained with hematoxylin-eosin illustrating a necrotic process and accumulation of inflammatory cells. *Panel B*, Silver staining of the same tissue from panel A. Note the collapse and disarray of the reticular framework (arrows). *Panel C*, Hematoxylin-eosin-stained tissue illustrating a periarteritis process. Note the adventitial lymphomononuclear inflammatory exudate and edema. Magnification bar: 500 µm.

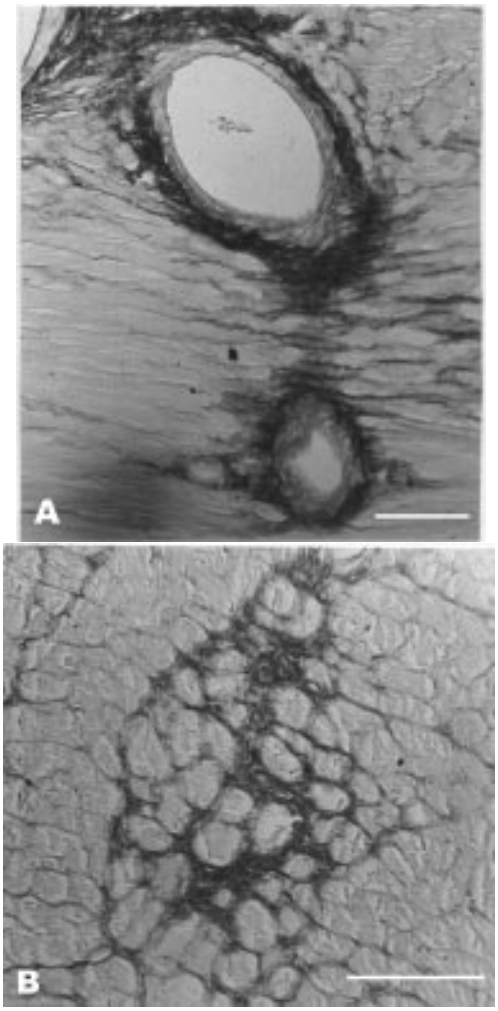

Figure 3 - Photomicrographs of rat myocardium after 8 weeks of renovascular hypertension. Panels A and B illustrate increased perivascular and pericellular fibrosis, and scarring (dark-stained collagen). Magnification bar: 500 µm; Sirius Red F3BA staining.

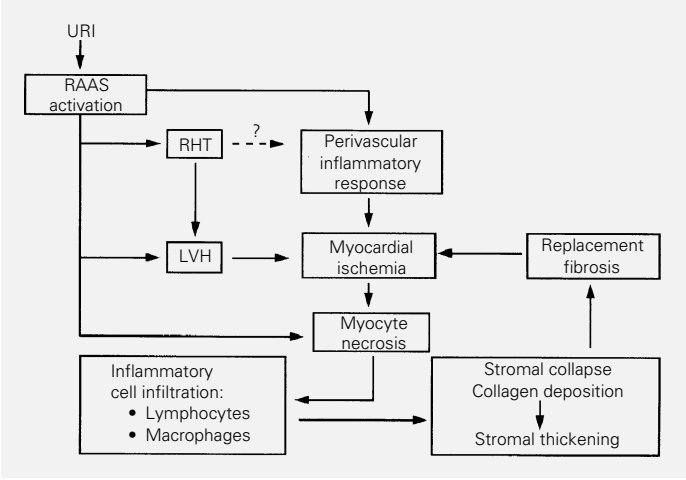

Figure 4 - Diagrammatic representation of a hypothesis for the physiopathology of myocardial fibrosis in renovascular hypertension. URI, Unilateral renal ischemia; RAAS, renin-angiotensin-aldosterone system; RHT, renovascular hypertension; LVH, left ventricular hypertrophy.

Before this, the myocardial function was normal, even in the presence of significant morphological changes. Accordingly, Cicogna et al. (15) induced expressive myocardial fibrosis in normotensive rats by chronic administration of colchicine and found unimpaired myocardial function, as analyzed in the isolated papillary muscle preparation. These results suggest that, in the experimental models of chronic heart damage, morphological changes precede myocardial dysfunction. However, it is necessary to remember that studies of systolic function in renovascular (33) or spontaneously hypertensive rats (34) have revealed that the myocardium can present a better systolic function than in normotensive control rats. Thus, the apparent normal results obtained in this study may in fact indicate impaired systolic function.

In the pressure overload hypertrophy, the relation between myocardial fibrosis and diastolic dysfunction has been previously described (11,12,35). In the present study, it was interesting to find increased myocardial passive stiffness in the RHT4 group, which had normal HOP concentration, and normal passive stiffness in the RHT8 group, which had increased myocardial HOP concentration. One possible explanation for this observation may be the qualitative changes of the myocardial collagen content. The RHT4 group had an increased accumulation of argyrophilic reticular fibers in areas of myocyte loss rather than replacement collagen fibrosis. The reticular fibers consist mainly of collagen type III, fibronectin and one or more non-collagenous glycoproteins (36), whereas replacement fibrosis consists mainly of type I collagen (37). Therefore, one would expect a decreased type I:III ratio early after myocyte necrosis. This imbalance may promote the diastolic dysfunction in the RHT4 group. In fact, Mukherjee and Sen (38) hypothesized that the type of collagen, rather than the total amount, might influence myocardial function.

In conclusion, the Goldblatt II model of renovascular hypertension in rats caused myocyte necrosis and arteriolar remodeling followed by fibrosis. Despite the extensive morphological changes, myocardial function remained close to normal.

Acknowledgments

The authors thank José Carlos Georgette and Vitor de Souza for technical assistance and Mario Augusto Dallaqua for secretarial assistance.

References

1. Capasso JM, Strobeck JE & Sonnenblick EH (1981). Myocardial mechanical alterations during gradual onset long-term hypertension in rats. *American Journal of Physiology*, 241: H435-H441.
2. Bing OHL, Wiegner AW, Brooks WW, Fishbein MC & Pfeffer JM (1988). Papillary muscle structure-function relations in the aging spontaneously hypertensive rat. *Clinical and Experimental Hypertension*, 10: 37-58.
3. Wisenbaugh T, Allen P, Cooper IV G, Holzgrefe H, Beller G & Carabello B (1983). Contractile function, myosin ATPase activity and isozymes in the hypertrophied pig left ventricle after a chronic progressive pressure overload. *Circulation Research*, 53: 332-341.
4. Capasso JM, Malhotra A, Scheuer J & Sonnenblick EH (1986). Myocardial, biochemical, contractile, and electrical performance after imposition of hypertension in young and old rats. *Circulation Research*, 58: 445-460.
5. Cohen ME & Bing OHL (1987). Performance of papillary muscles from the aging spontaneously hypertensive rat: temporal changes in isometric contraction parameters. *Proceedings of the Society for Experimental Biology and Medicine*, 185: 318-324.
6. Williams Jr JF, Mathew B, Hern DL & Potter RD (1983). Myocardial hydroxyproline and mechanical response to prolonged pressure loading followed by unloading in the cat. *Journal of Clinical Investigation*, 72: 1910-1917.
7. Lecarpentier Y, Bugaisky LB, Chemla D, Mercadier JJ, Schwartz K, Whalen RG & Martin JL (1987). Coordinated changes in contractility, energetics, and isomyosins after aortic stenosis. *American Journal of Physiology*, 252: H275-H282.
8. Weber KT, Pick R, Jalil JE, Janicki JS & Carrol EP (1989). Patterns of myocardial fibrosis. *Journal of Molecular and Cellular Cardiology*, 21 (Suppl V): 121-131.
9. Conrad CH, Brooks WW, Robinson KG & Bing OHL (1991). Impaired myocardial function in spontaneously hypertensive rats with heart failure. *American Journal of Physiology*, 260: H136-H145.
10. Bing OHL, Brooks WW, Robinson KG, Slawsky MT, Hayes JA, Litwin SE, Sen S & Conrad CH (1995). The spontaneously hypertensive rat as a model of the transition from compensated left ventricular hypertrophy to failure. *Journal of Molecular and Cellular Cardiology*, 27: 383-396.
11. Thiedemann K-U, Holubarsch Ch, Medugorac I & Jacob R (1983). Connective tissue content and myocardial stiffness in pressure overload hypertrophy. A combined study of morphologic, morphometric, biochemical, and mechanical parameters. *Basic Research in Cardiology*, 78: 140-155.
12. Doering CW, Jalil JE, Janicki JS, Pick R, Aghili S, Abrahams G & Weber KT (1988). Collagen network remodelling and diastolic stiffness of the rat left ventricle with pressure overload hypertrophy. *Cardiovascular Research*, 22: 686-695.
13. Jalil JE, Janicki JS, Pick R & Weber KT (1991). Coronary vascular remodeling and myocardial fibrosis in the rat with renovascular hypertension. Response to captopril. *American Journal of Hypertension*, 4: 51-55.
14. Hinglais N, Heudes D, Nicoletti A, Mandet C, Laurent M, Bariéty J & Michel J-B (1994). Colocalization of myocardial fibrosis and inflammatory cells in rats. *Laboratory Investigation*, 70: 286-294.
15. Cicogna AC, Brooks WW, Hayes JA, Robinson KG, Sen S, Conrad CH & Bing OHL (1997). Effect of chronic colchicine administration on the myocardium of the aging spontaneously hypertensive rat. *Molecular and Cellular Biochemistry*, 166: 45-54.
16. Weber KT, Janicki JS, Pick R, Capasso J & Anversa P (1990). Myocardial fibrosis and pathologic hypertrophy in the rat with renovascular hypertension. *American Journal of Cardiology*, 65: 1G-7G.
17. Tan LB, Jalil JE, Pick R, Janicki JS & Weber KT (1991). Cardiac myocyte necrosis induced by angiotensin II. *Circulation Research*, 69: 1185-1195.
18. Kabour A, Henegar JR & Janicki JS (1994). Angiotensin II (AII)-induced myocyte necrosis: role of the AII receptor. *Journal of Cardiovascular Pharmacology*, 23: 547-553.
19. Kabour A, Henegar JR, Devineni VR & Janicki JS (1995). Prevention of angiotensin II induced myocyte necrosis and coronary vascular damage by lisinopril and losartan in the rat. *Cardiovascular Research*, 29: 543-548.
20. Rodrigues MAM, Bregagnollo EA, Montenegro MR & Tucci PJF (1992). Coronary vascular and myocardial lesions due to experimental constriction of the abdominal aorta. *International Journal of Cardiology*, 35: 333-341.
21. Jalil JE, Doering CW, Janicki JS, Pick R, Shroff SG & Weber KT (1989). Fibrillar collagen and myocardial stiffness in the intact hypertrophied rat left ventricle. *Circulation Research*, 64: 1041-1050.
22. Campbell SE, Janicki JS & Weber KT (1995). Temporal differences in fibroblast proliferation and phenotype expression in response to chronic administration of angiotensin II or aldosterone. *Journal of Molecular and Cellular Cardiology*, 27: 1545-1560.

23. Switzer BR (1991). Determination of hydroxyproline in tissue. *Journal of Nutritional Biochemistry*, 2: 229-321.
24. Ratkowsky DA (Editor) (1983). Comparing parameter estimates from more than one data set. In: *Nonlinear Regression Modelling; a Unified and Practical Approach*. Dekker, New York, 135-152.
25. Hirsch AT, Talsnec CE, Schunkert H, Paul M & Dzau VT (1991). Tissue specific activation of cardiac angiotensin converting enzyme in experimental heart failure. *Circulation Research*, 69: 475-482.
26. Ratajska A, Campbell SE, Sun Y & Weber KT (1994). Angiotensin II-associated cardiac myocyte necrosis: role of adrenal catecholamines. *Cardiovascular Research*, 28: 684-690.
27. Ratajska A, Campbell SE, Cleutjens JPM & Weber KT (1994). Angiotensin II and structural remodeling of coronary vessels in rats. *Journal of Laboratory and Clinical Medicine*, 124: 408-415.
28. Giacomelli F, Anversa P & Wiener J (1976). Effect of angiotensin-induced hypertension on rat coronary arteries and myocardium. *American Journal of Pathology*, 84: 111-125.
29. Laine GA & Allen SJ (1991). Left ventricular myocardial edema: lymph flow, interstitial fibrosis and cardiac function. *Circulation Research*, 68: 1713-1721.
30. Sigusch HH, Ou R, Katwa LC, Campbell SE, Ganjam VK, Reddy HK & Weber KT (1995). Angiotensin-II-induced increase in transcoronary protein clearance: role of hypertension *vs* nitric oxide or cyclo-oxygenase products. *Cardiovascular Research*, 30: 291-298.
31. Sigusch HH, Campbell SE & Weber KT (1996). Angiotensin II-induced myocardial fibrosis in rats: role of nitric oxide, prostaglandins and bradykinin. *Cardiovascular Research*, 31: 546-554.
32. Conrad CH, Brooks WW, Hayes JA, Sen S, Robinson KG & Bing OHL (1995). Myocardial fibrosis and stiffness with hypertrophy and heart failure in the spontaneously hypertensive rat. *Circulation*, 91: 161-170.
33. de Simone G, Deveraux RB, Volpe M, Camargo MJ, Wallerson DC & Laragh JH (1992). Relation of left ventricular hypertrophy afterload, and contractility to left ventricular performance in Goldblatt hypertension. *American Journal of Hypertension*, 5: 292-301.
34. Bing OHL, Sen S, Conrad CH & Brooks WW (1984). Myocardial function structure and collagen in the spontaneously hypertensive rat: progression from compensated hypertrophy to haemodynamic impairment. *European Heart Journal*, 5 (Suppl F): 43-52.
35. Holubarsch Ch (1980). Contracture type and fibrosis type of decreased myocardial distensibility. Different changes in elasticity of myocardium in hypoxia and hypertrophy. *Basic Research in Cardiology*, 75: 244-252.
36. Unsworth DJ, Scott DL, Almond TJ, Beard HK, Holborow EJ & Walton KW (1982). Studies on reticulin. I: Serological and immunohistological investigation of the occurrence of collagen type III, fibronectin and the non-collagenous glycoprotein of pras and glynn in reticulin. *British Journal of Experimental Pathology*, 63: 154-166.
37. Weber KT, Janicki JS, Shroff SG, Pick R, Chen RM & Bashey RI (1988). Collagen remodeling of the pressure-overloaded, hypertrophied nonhuman primate myocardium. *Circulation Research*, 62: 757-765.
38. Mukherjee D & Sen S (1990). Collagen phenotypes during development and regression of myocardial hypertrophy in spontaneously hypertensive rats. *Circulation Research*, 67: 1474-1480.